Analytical Methods

Volume 1 | Number 1 | Jan 2013 | Pages 1–100

Analytical Methods

www.rsc.org/methods

ROYAL SOCIETY OF CHEMISTRY

www.rsc.org/methods

A GMI biochip platform based on Co-based amorphous ribbon for detection of magnetic Dynabeads

Zhen Yang*, Chong Lei, Yong Zhou*, Yan Liu and Xue-cheng Sun

We describe a giant magnetoimpedance (GMI) biochip platform for detection of streptavidin-coupled magnetic Dynabeads with different size. The GMI sensor based on micro-patterned Co-based amorphous ribbons (Metglas® 2714A) with a meander structure was fabricated by micro-electro-mechanical-system (MEMS) technology. A gold film was then deposited on the GMI element to act as a support platform for immobilizing various concentrations of magnetic Dynabeads (1 μm and 2.8 μm). The results indicated that Dynabeads of 1 μm in diameter with a concentration as low as 5 μg/ml can be detected by using the ribbon-based GMI sensor, and detection limit for Dynabeads of 2.8 μm was 1 μg/ml. Besides, using same number of magnetic Dynabeads with different size, the GMI responses were significantly enhanced after coating 2.8 μm Dynabead. The ribbon-based micro-integrated GMI biosensor is easy to fabricate and expected to be used for detection of a very low concentration of Dynabeads-labeled biomarkers.

1. Introduction

Magnetic biodetection methods based on micro-sized magnetic beads was proposed in 1998 by Baselt [1]. Since then, magnetic beads have been gradually introduced into cell biology and molecular biology due to a wide range of applications in biotechnology and biomedicine, including magnetic nucleic acid isolation [2], immunoassay [3], disease diagnoses [4] and targeted drug delivery [5]. The important requirements of a magnetic biosensor regarding the detection of magnetic beads include high sensitivity, low power consumption, quick response, reliability, environment-friendly operation, and low cost.

Magnetic sensors relying on various principles, such as giant magnetoresistance (GMR) and superconducting quantum interference device (SQUID) [6] have been developed to detect magnetic beads. However, a well known shortcoming of GMR sensors is their limited sensitivity, which is less than 2%/Oe with respect to the applied magnetic field [7-9], and SQUID sensors require extremely low temperatures for operation. By contrary,

giant magneto-impedance GMI sensors are more sensitive (100%/Oe) to low magnetic fields and present smaller power dissipation per unit area [10]. The GMI effect consists of a large variation in real and imaginary components of impedance (Z) of a conductive magnetic specimen while high-frequency AC current flows through it and sample is subjected to DC magnetic field [11-12]. The effect has been mostly observed in rectangular and cylindrical geometries, such as micro-wires [13-14] films [15-16] and ribbons [17-18] of different soft ferromagnetic materials. Among them, Co-based amorphous ribbons with nearly vanishing magnetostriction ($\lambda \sim 0$) have been reported to exhibit GMI effects with a high degree of field sensitivity and are therefore promising candidate materials for making advanced magnetic sensors [19].

In recent years, detection of magnetic beads based on GMI effect have been presented constantly. A GMI-biosensor fabricated using an amorphous ribbon was employed to detect magnetic Dynabeads® M-450 [20]. Flexible NiFe/Cu/NiFe multilayered GMI biosensors were presented to detect the Dynabeads protein A and streptavidin-coupled Dynabeads [21-23]. Detection of magnetic-particle concentration in continuous flow based in GMI effect was performed [24]. A GMI biosensor based on Co-based amorphous ribbon was designed and tested to detect functionalized Nanomag-D magnetic beads [25]. Moreover, the ribbon

Key Laboratory for Thin Film and Microfabrication Technology, Department of Micro/Nano Electronics, School of electronic information and electrical engineering, Shanghai Jiao Tong University, Dongchuan Road 800, Shanghai, China. Tel: +86-21-34204315; Fax: +86-21-34204312; E-mail: zhc025@sjtu.edu.cn (Z. Yang); E-mail: yzhou@sjtu.edu.cn (Y. Zhou)

1

GMI sensors combined with magnetic particles were used for detection of viruses and cells in order to develop a new generation of biosensing system for biological recognition and selective detection [26, 27].

The goal of this work is to establish a GMI biochip platform based on micro-patterned Co-based amorphous ribbons for detection of streptavidin-coupled magnetic Dynabeads with different size (1 μm and 2.8 μm). The ribbon-based GMI sensor was fabricated by micro-electro-mechanical-system (MEMS) technology. Au film was integrated into ribbon-based GMI sensor for potential biochemical binding function, and detection of Dynabeads was performed on Au film of the ribbon-based GMI sensor. Overall, the studies demonstrate the possibility of using a ribbon-based micro-integrated GMI biosensor for highly sensitive detection of magnetic Dynabeads-labeled biological components.

2. Experimental details

2.1 Soft magnetic material and magnetic beads

Co-based commercial amorphous ribbons (Metglas® 2714A) with 20μm in thickness and 50mm in width is purchased from Metglas Company. Two types of solutions containing magnetic Dynabeads are purchased from Invitrogen and have been used. One is Dynabeads® MyoneTM streptavidin C1 (superparamagnetic beads of 1 μm in diameter) containing 10 mg/mL of magnetic beads (~7–10 × 10^8 beads/mL) in phosphate buffered saline (PBS) pH 7.4, with 0.01% Tween®-20 and 0.09% sodium azide as a preservative. The other is Dynabeads® M-280 Streptavidin (superparamagnetic beads of 2.8 μm in diameter) containing 10 mg (~6–7 × 10^8) Dynabeads®/mL in phosphate buffered saline (PBS) pH 7.4, with 0.1% bovine serum albumin (BSA) and 0.02% sodium azide as preservatives. Dynabeads are polymeric microspheres synthesized by γ-Fe_2O_3 and Fe_3O_4. Each micro bead is coated by a layer of polymeric material so that it can serve as an absorption and combination carrier of a variety of molecules. Due to the uniformity of volume and shape, biological activity, and affinity for biotin and superparamagnetism, Dynabeads show a brilliant application prospect in the field of biology.

2.2 Design and fabrication of GMI sensor

The GMI biochip platform based on Co-based amorphous ribbon was fabricated by micro-electro-mechanical-systems (MEMS) technology. Before MEMS processing, the ribbons were subjected to annealing treatment in 200 Oe magnetic field at 380 ℃ in a vacuum oven to induce transverse anisotropy. The annealing process was reported in our previous work [28]. The ribbons with magnetic field-annealed were designed and patterned into a meander structure with width of 500 μm, length of 5 mm, intervals of 60 μm and three turns (each 'n' shape in the meander structures was called one turn). The total area of sensing elements is 5 mm × 3.3 mm.
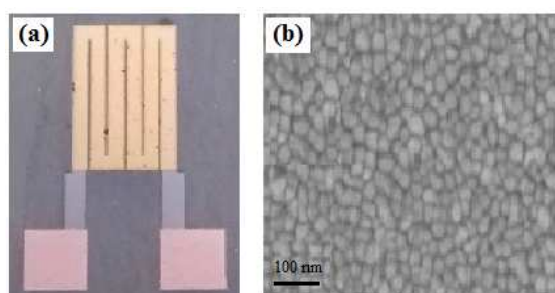
Fig. 1 The top view of fabricated micro-patterned Co-based amorphous ribbons integrated with an Au film (a) and the nano-Au film serves as the biosensing platform (b).

Fig. 1 showed the top views of the GMI biochip platform and scanning electron microscope (SEM) image of nano-Au film. The manufacturing processes of GMI biochip platform consisted of the following steps: 1, Co-based ribbon with magnetic field-annealed was tightly attached to Si substrate by epoxy adhesive; 2, photoresist was spun on ribbon with the thickness of 15 μm, and then the ribbon was patterned with a mask by UV lithography; 3, the ribbon was etched in acidic mixed solution (HNO_3: HCl: H_2O_2: H_2O= 1:2:4:8) for 5 min. The error of ±2.5 μm was found after etching process and it was considered to be acceptable with the comparatively large size of the structures; 4, the photoresist was removed; 5, polyimide was then spun on the wafer to fill the space between neighbor segments. To avoid the adverse effects of the nonuniform surface caused by spinning polyimide (PI) on the surface of the sensor, the polyimide layer was baked at 250 ℃ for 2h in low vacuum; 6, polyimide
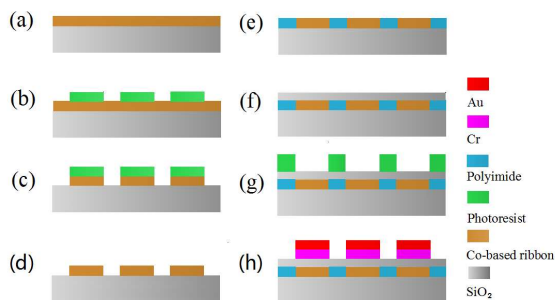
Fig. 2 Fabrication steps of the ribbon-based GMI sensor integrated with an Au film.

was polished until the GMI sensing element was exposed out; 7, Cr/Cu seed layer with the thickness of 100nm was deposited on patterned ribbon by RF sputtering. 1 mm×1 mm Cu electrodes with thickness of 20 μm were electroplated; 8, the seed layer was removed by reactive iron etching method. 9, SiO$_2$ thin film with the thickness of 200 nm was deposited upon sensing element as an insulative and protective layer; 10, photoresist was spun on ribbon with the thickness of 15 μm and then was exposed by UV lithography; 11, the Cr/Au films with a thickness of 300 nm were sputtered on the SiO2 layer, and then the photoresist was removed. Fig. 2 showed the fabrication steps of the Co-based ribbon GMI sensor.

2.3　Experimental procedure

Two ribbon GMI sensor (sensor A and sensor B) were used for detection of magnetic Dynabeads with different size. Before immobilization of Dynabeads, the ribbon

GMI sensors were bathed in 1 mol/l NaOH solution and 1 mol/l HCl in turn for 10 min, and then the sensors were rinsed with deionized water and alcohol, at last they were dried using a stream of nitrogen gas. Dynabeads® C1 and M-280 were diluted in PBS to obtain 1 μg/ml, 5 μg/ml, 10 μg/ml and 100 μg/ml magnetic Dynabeads. We take 7 × 108 particles per milliliter for Dynabeads® C1 and 7 × 108 particles per milliliter for Dynabeads® M-280 as the calculation standard, so 10 μl of 1 μg/ml of Dynabeads® C1 and 1 μg/ml of Dynabeads® M-280 contain 700 particles, respectively. 10 μl of Dynabeads® C1 and Dynabeads® M-280 with different concentrations were dropped on sensor A and sensor B, respectively, then the GMI sensors were stored in a well-closed container at 4 ℃ for 24 h for the adsorption reaction.

The GMI effect of the micro-patterned ribbon was measured by an impedance analyzer (HP4194A). The longitudinal external field (H$_{ex}$) was generated by a direct current (DC) field source (0–120 Oe) and was applied along the longitudinal direction of the sample in order to induce strong changes in the skin depth. The GMI ratios without magnetic Dynabeads were treated as datum value. The relative change in impedance (GMI ratio) was defined as: GMI ratio (100%) =100 % × $[Z(H)-Z(H_{max})]/Z(H_{max})$, where $Z(H_{max})$ was the magnetoimpedance with 120 Oe. The test setup was shown in Fig. 3.
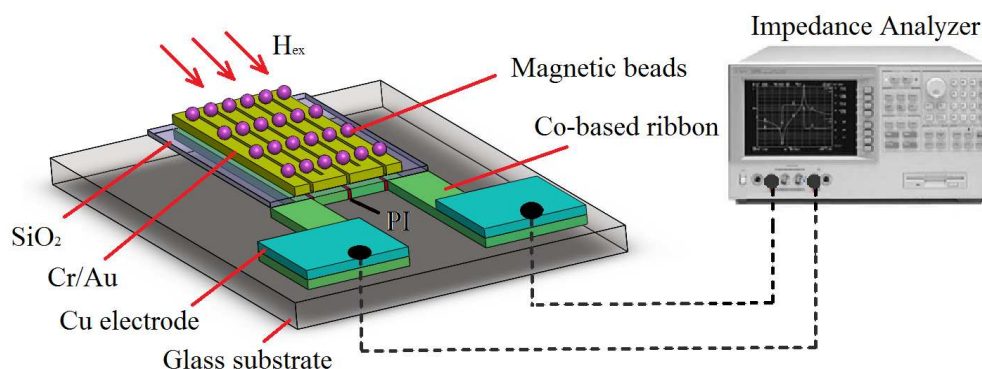
Fig. 3 The GMI-based biosensing platform for the detection of magnetic Dynabeads
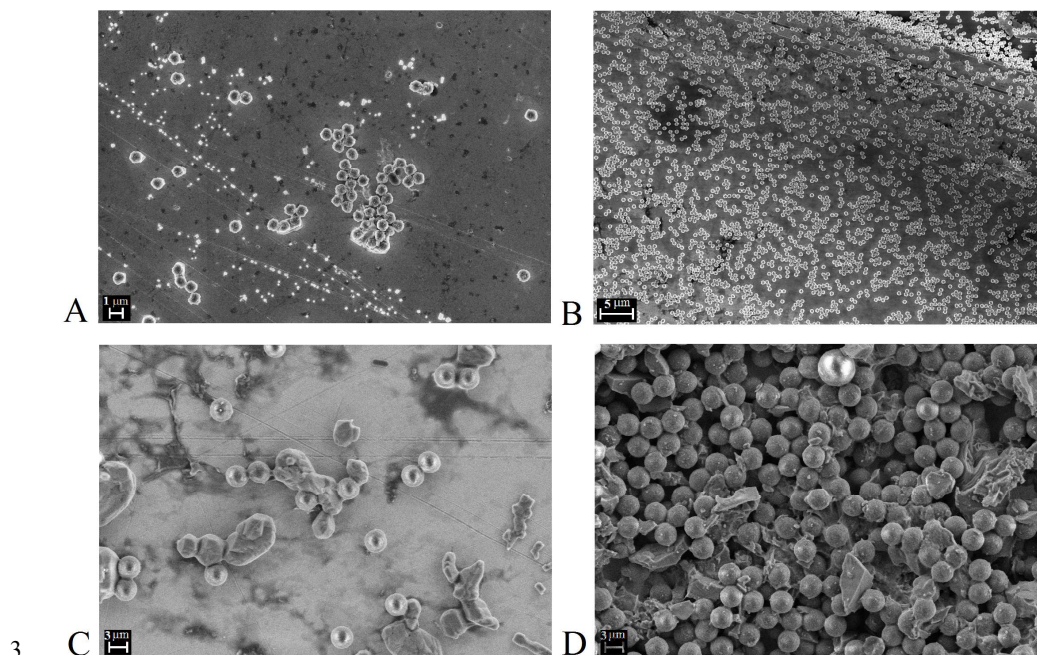
Fig. 4 SEM photographs of Dynabeads® C1 (A) 1 µg/ml; (B) 100 µg/ml; and Dynabeads® M-280 (C) 1 µg/ml; (D) 100 µg/ml

3. Results and discussion

3.1 Characterization of magnetic Dynabeads

Scanning electron microscopy (SEM) was used to observe the Dynabeads® C1 and Dynabeads® M-280 at concentrations of 1 µg/ml and 100 µg/ml as seen in Fig. 4. We can find that low concentration Dynabeads (1 µg/ml) disperse uniformly on the whole Au film (see Fig. 4 A and C), however high-concentration dosage (100 µg/ml) cause uneven distributions and high-density clusters of Dynabeads (see Fig. 4 B and D). Compared with Fig. 4 B and D, we can see that clustering degree for 2.8 µm Dynabeads is more obvious (see Fig. 4 D). The SEM observations confirmed that Dynabeads was immobilized on the Au film.

3.2 Detection of magnetic Dynabeads

The magnetic-field dependence and AC frequency dependence of the GMI ratio of the ribbon coated without and with different Dynabeads® C1 concentrations are shown in Fig. 5. Evidently, the GMI ratio has risen in varying degrees due to the presence of different concentrations of Dynabeads® C1. And we can find that the GMI responses of ribbon coated without Dynabeads® C1 and with Dynabeads® C1 at concentration of 1 µg/ml are almost the same (a slight rise). It is meant that Dynabeads® C1 with a concentration as low as 1 µg/ml cannot be detected by the GMI biochip platform. When the high concentration Dynabeads® C1 (5-100 µg/ml) are immobilized on the Au platform, the GMI ratio have significant difference. Moreover, the rise of GMI ratio increases with increasing Dynabeads® C1 concentration. When the Dynabeads with 5 µg/ml, 10 µg/ml and 100 µg/ml are immobilized, the increases are 2.71%, 5.03 % and 8.13 %, respectively. The obtained results are different from our previous results [22], lower detection sensitivity of 5 µg/ml is acquired in the work and GMI responses don't fall at high concentration Dynabeads® C1. In our view, the magnetic field sensitivity of the ribbon is the main reason. It is worthwhile to note that the GMI ratios increase with the external field H_{ex} up to about 20 Oe and then shows a sharp drop as H_{ex} continues to increase as shown in Fig. 5 (a). This can be explained in terms of magnetization rotation model [11]: the rotational magnetic permeability related to the GMI effect is first increased and then decreased with increasing H_{ex}, the maximum permeability is achieved as $H_{ex}=H_k$.

(a)

(b)
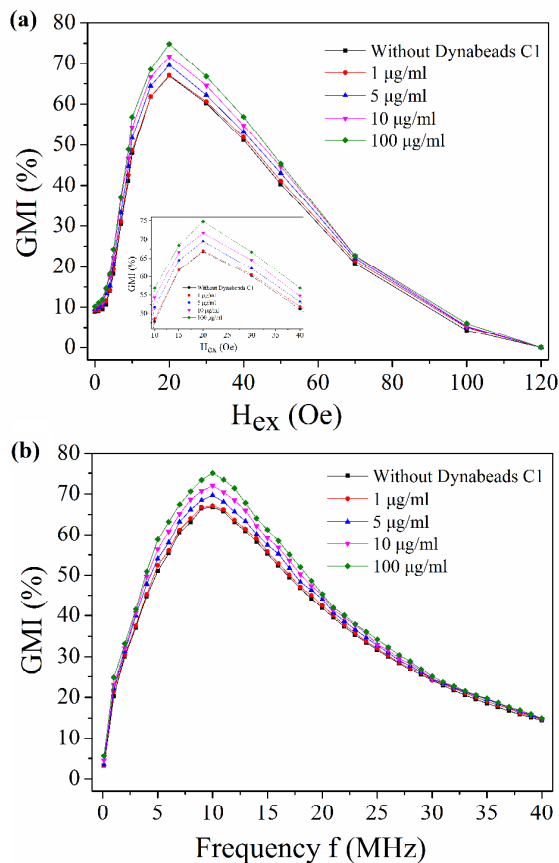
Fig. 5 (a) Magnetic-field and (b) AC-frequency dependence of the GMI ratio of the ribbon coated with different Dynabeads[®] C1 concentrations. (a) Inset: magnetic-field dependence of GMI response obtained near the anisotropy

H_k is the anisotropy field. The inset of Fig. 5 (a) shows that the stronger GMI response are obtained near the H_k. In our early reports [22, 29], the GMI ratio was improved owing to the presence of superparamagnetic beads on the surface of the sensor, and it was found that high field sensitivity in detection of magnetic beads can be obtained near H_k. At low magnetic fields, Dynabeads are magnetizes at a low level and the sensor has low field sensitivity. Under overlarge magnetic fields, the stray magnetic field of Dynabeads becomes strongly overwhelmed. The present result is in agreement with it. Many similar researches were also reported previously [25, 30], and related theories were put forward to explain the phenomenon. In addition, there is a small change of the GMI ratio at lower frequency but large change of the

GMI ratio occurs at high frequency. The greatest change of GMI ratio has taken place near the frequency at which the GMI ratio reaches the maximum (f = 10 MHz) as shown in Fig. 5 (b). Therefore, the ribbon GMI sensor has higher sensitivity in detecting Dynabeads at a frequencies of 10 MHz. The GMI responses begin to fall with the further increasing of frequency. This is because that the GMI effect originates mainly from the skin effect owing to a strong change in the effective permeability causes by the applied DC magnetic field. In the case of small skin effect at low frequency, the sensing element is insensitive to the fringe field. However, both the domain wall motion and magnetic moment rotation contributed to the transverse permeability at high frequency. With the further increase of frequency, domain wall motion becomes strongly damped by the eddy currents [11].

Fig. 6 shows the magnetic-field and AC-frequency

(a)

(b)
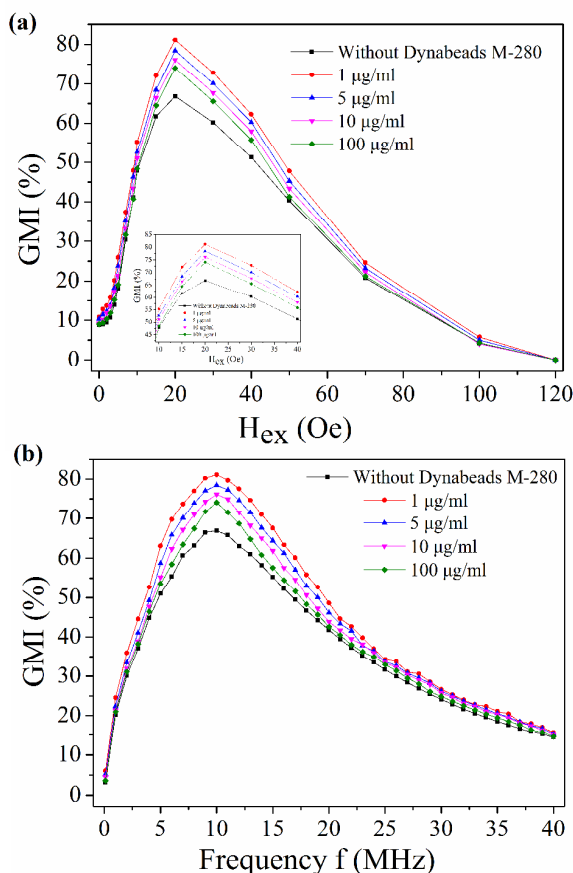
Fig. 6 (a) Magnetic-field and (b) AC-frequency dependence of the GMI ratio of the ribbon coated with different Dynabeads[®] M-280 concentrations. (a) Inset:
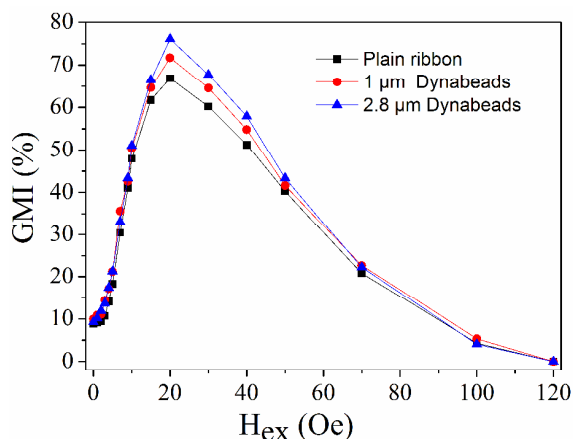
Fig. 7 GMI responses of the Co-based amorphous ribbon in presence of Dynabeads® C1 and Dynabeads® M-280 with the same number (7000 beads/ml).

dependence of the GMI ratio of the ribbon coated with different Dynabeads® M-280 concentrations. Similarly, we find that GMI ratio has risen in varying degrees due to the presence of different concentrations of Dynabeads® magnetic-field dependence of GMI response obtained near the anisotropy M-280. However, unlike the preceding results, the GMI ratio first increases and then decreases with increasing Dynabeads® M-280 concentration as shown in Fig. 6 (a) (inset). In our early study [23], we indicated that high concentration Dynabeads could also cause the high-density clusters of Dynabeads, and enabling the adjacent exciting fields of Dynabeads to cancel each other out, the fringe field was therefore reduced. And there is a 14.11% increase in GMI ratio at f= 10 MHz under the condition of 1μg/ml Dynabeads® M-280, which shows the maximum detection sensitivity. It is lower than 0.1 μg/ml that obtained in previous work [16, 18]. This may be still related to the the magnetic field sensitivity of the ribbon. The magnetic-field dependence and frequency dependence of the GMI ratio of the ribbons has the same variation trend compared with Fig. 5, so the same explanation of the mechanism can be presented mentioned above. The GMI responses of each field point as well as frequency point have been measured for 5 times on a Dynabeads concentration, the GMI sensor shows attractive reproducibility of each field point as well as frequency point with low relative standard deviation of less than

0.86%.

The fabricated ribbon GMI sensors have nearly the same magnetic properties. To better illustrate the relative change in GMI due to the presence of magnetic Dynabeads® C1 and Dynabeads® M-280, we display in Fig. 7, the magnetic-field dependence of the maximum GMI ratios for the ribbons A and B coated with the same number Dynabeads (7×10^3 beads/ml). It is very interesting to note that relative to the plain ribbon, the presence of the Dynabeads® M-280 significantly increases the GMI ratio for the ribbon. At f= 10 MHz, the GMI increases from 66.86% for the plain ribbon to 76.12% for the ribbon coated with 7000 Dynabeads® M-280 (10 μl of 10 μg/ml). However, there is a smaller change (71.73%- 66.86%= 4.87%) of the GMI ratio for the ribbon coated with 7×10^3 Dynabeads® C1 (10 μl of 10 μg/ml). That is to say that the GMI response signal is more obvious for 2.8 μm Dynabead. Simultaneously, it is noted that the GMI ratio (74.1%) of ribbon coated with 7×10^4 Dynabeads® M-280 (10 μl of 100 μg/ml) is slightly lower than that (74.82%) coated with 7×10^4 Dynabeads® C1 (10 μl of 100 μg/ml). The reason is that high concentration Dynabeads could also cause the high-density clusters of Dynabeads (see Fig. 4 B and D) mentioned above. The influences of particles size on the GMI and field sensitivity have been investigated systematically by Laurita [30]. The present results is in good agreement with it.

Two primary kinds of viewpoint were used to explain the phenomenon of GMI enhancement. One is that the majority of magnetic nanoparticles is magnetized by the transverse AC field in the transverse direction, the coupling of the stray field of the magnetic beads with the transverse AC field increase the transverse permeability, thereby causing high change in the impedance [25]. Another is that the presence of the magnetic particles may change the superposition of the constant applied field and the alternating field, thereby changing the magnetic charge distribution near the surface of the sensing element, the GMI effect is thus enhanced [31]. In our previous work [22], the pinning effect of superparamagnetic beads on the sensing elements was put forward to explain the reason for enhancement in GMI effect. It is considered that the Dynabeads pinning field

may inhibit the domain wall motion but strengthen the magnetic moment's rotation, and the rotational magnetic permeability of the sensing elements is modified by the fringe field, which contributes to the enhanced GMI effect accordingly.

Though the detection sensitivity for Dynabeads is lower than that in the previous studies [21-23], the fabrication process of ribbon-based GMI sensor is simpler. Enhancement of the GMI effect in Co-based amorphous ribbons can be achieved by coating with copper, zinc oxide, diamagnetic organic thin film, cobalt, or carbon nanotubes [32-36], applying tensile stress [37], annealing treatment [38] and appropriate geometries [28]. So in theory the detection limit for Dynabeads detection could be improved by using highly sensitivity ribbon GMI biosensor. Treating the surface of a ribbon with an appropriate concentration of acid is also shown to improve the sensitivity of detection of a ribbon-based GMI biosensor [25]. The ribbon-based GMI biosensor is of considerable interest due to potential application in the biomedical field of various specific detection.

4. Conclusion

Micro-patterned GMI sensing elements were prepared from a cobalt-based commercial amorphous ribbon (Metglas® 2714A) using micro electro-mechanical system (MEMS) technology. A gold film was then deposited on the GMI sensing element to act as a support for biosensing platform. Detection of streptavidin-coupled magnetic Dynabeads® C1 and Dynabeads® M-280 by using the micro-integrated GMI sensor was accomplished. Dynabeads® C1 (1 μm in diameter) with a concentration as low as 5 μg/ml (3500 Dynabeads) can be detected by using the ribbon-based GMI sensor, and detection limit for Dynabeads® M-280 (2.8 μm) was 1 μg/ml (700 Dynabeads). According to the previous reports [21-23], 90 Dynabeads can be detected by using NiFe/Cu/NiFe multilayered GMI sensor. Detection limit for Dynabeads® C1 and Dynabeads® M-280 detection could be improved by using more sensitive ribbon GMI sensor. Besides, using same number of magnetic Dynabeads with different size, the GMI responses were significantly enhanced after coating 2.8 μm Dynabead. Though the detection sensitivity for Dynabeads is lower, the ribbon-based

micro-integrated GMI biosensor is easy to fabricate and expected to be used for detection of a very low concentration of Dynabeads-labeled biomarkers.

Acknowledgments

References

1 D. R. Baselt, G. U. Lee, M. Natesan, S. W. Metzger, P. E. Sheehan and R. Colton, Biosens. Bioelectron., 1998, 13, 731-739.

2 J. Oster, J. Parker and L. à Brassard, J. Magn. Magn. Mater., 2001, 225, 145-150.

3 A. Fan, C. Lau and J. Lu, Anal. Chem., 2005, 77, 3238–42.

4 T. Aytur, J. Foley, M. Anwar, B. Boser, E. Harris and P. Robert Beatty, J. Immunol. Methods, 2006, 314, 21–29.

5 M. L. H. Gruwel, Y. Yang, P. de Gervai, J. Sun and V. V. Kupriyanov, Magn. Reson. Imaging, 2009, 27, 70–977

6 D. Drung, C. Assmann, J. Beyer, A. Kirste, M. Peters, F. Ruede, and T. Schurig, IEEE Trans. Appl. Supercond., 2007, 17, 699–704

7 H. A. Ferreira, D. L. Graham, P. P. Freitas, and J. M. S. Cabral, J. Appl. Phys. 2003, 93, 7281-7286

8 D. L. Graham, H. A. Ferreira, and P. P. Freitas, Trends Biotechnol. 2004, 22, 455-462

9 D. L. Graham, H. A. Ferreira, P. P. Freitas, and J. M. S. Cabral, Biosens. Bioelectron. 2003, 18, 483-488

10 Y. Nishibe, H. Yamadera, N. Ohta, K. Tsukada, and Y. Nomomura, Sens. Actuators A 2000, 82, 155

11 L. V. Panina and K. Mohri, Appl. Phys. Lett., 1994, 65, 1189.

12 M. H. Phan and H. X. Peng, Prog. Mater. Sci., 2008, 53, 323.

13 F. E. Atalay, H. Kaya and S. Atalay, J. Phys. D, Appl. Phys., 2006, 39, 431.

14 M. Vázquez, M. Knobel and M. L. Sánchez, Sens. actuators A., 1997, 159, 20-29.

15 R. L. Sommer and C. L. Chine, Appl. Phys. Lett., 1995, 47, 3346.

16 Y. Zhou, J. Q. Yu, X. L. Zhao and B. C. Cai, J. Appl. Phys., 2001, 89, 1816-1819.

17 F. Alves, L. Abi Rached, J. Moutoussamy and C. Coillot, Sens. actuators A., 2008, 142459.

18 M. H. Phan, H. X. Peng, M. R. Wisnom, S. C. Yu, N. H. Nghi and C. G. Kim, Sens. actuators A., 2006, 129, 62.

19 L. Kraus, Sens. Actuators. A., 2003, 106, 187.

20 G. Kurlyandskaya and V. Levit, Biosens. Bioelectron., 2005, 20, 1611–1616.

21 T. Wang, Y. Zhou, C. Lei, J. Lei and Z. Yang, Sens Actuators B., 2013, 186, 727-733.

22 T. Wang, Z. Yang, C. Lei, J. Lei and Y. Zhou, Phys. status solidi A, 2014, 211(6), 1389-1394.

23 T. Wang, Y. Zhou, C. Lei, J. Lei and Z. Yang, Microchim Acta., 2013, 180, 1211-1216.

24 A. García-Arribas, F. Martínez and E. Fernández, Sens Actuators A., 2011, 172(1), 103-108.

25 J. Devkota, A. Ruiz and P. Mukherjee, IEEE Transactions on Magnetics., 2013, 49(7), 4060-4063.

26 L. Chen, C. C. Bao, H. Yang, C. Lei, Y. Zhou and D. X. Cui, Biosens. Bioelectron., 2011, 26, 3246–3253.

27 H. Yang, L. Chen, C. Lei and J. Zhang, Appl. Phys. Lett., 2010, 97(4), 043702.

28 Z. Yang, J. Lei, C. Lei, T. Wang and Y. Zhou, Applied Physics A, 2014, 1-5.

29 T. Wang, Z. Yang, C. Lei, J. Lei and Y. Zhou, Biosens. Bioelectron., 2014, 58, 338–344.

30 N. Laurita, A. Chaturvedi, K. Stojak, S. Chandra, M. H. Phan and H. Srikanth, In APS Meeting Abstracts 2011, March, (Vol. 1, p. 19009).

31 G. V. Kurlyandskaya, M. L. Sanchez, B. Hernando, V. M. Prida, P. Gorria and M. Tejedor, Appl. Phys. Lett., 2003, 82, 3053–3055.

32 A. A. Taysioglu, A. Peksoz, Y. Kaya, N. Derebasi, G. Irez and G. Kaynak, J. Alloys Compd., 2009, 487, 38.

33 A. A. Taysioglu, Y. Kaya, A. Peksoz, S. K. Akay, N. Derebasi, G. Irez and G. Kaynak, IEEE Trans. Magn., 2010, 46, 405.

34 A. Peksoz, Y. Kaya, A. A. Taysioglu, N. Derebasi and G. Kaynak, Sens. Actuators, A., 2010, 159, 69.

35 N. Laurita, A. Chaturvedi, C. Bauer, P. Jayathilaka, A. Leary, C. Miller, H. Srikanth, and M. H. Phan, J. Appl. Phys., 2011, 109, 07C706.

36 A. Chaturvedi, K. Stojak, N. Laurita, P. Mukherjee, H. Srikanth, and M. H. Phan, J. Appl. Phys., 2012, 111, 07E507.

37 M. Moradi, A. Dadsetan, S. M. Mohseni and A. J. Gharehbagh, Journal of Superconductivity and Novel Magnetism, 2015, 1-4.

38 F. Jin, L. Zhou, W. Cheng, Y. Zhang, B. Tong and Y. Xu, IEEE Trans. Magn., 2014, 50, 4400404.